

The CFHT Legacy Survey: The Morphology-Density Relation of Galaxies out to $z \sim 1$ ¹

Martijn J. H. M. Nuijten^{2,3,5}, Luc Simard³, Stephen Gwyn^{4,5}, Huub J. A. Röttgering²

ABSTRACT

We study the relationships between galaxy total luminosity ($M_{g'}$), morphology, color and environment as a function of redshift. We use a magnitude-limited sample of 65,624 galaxies in the redshift range $0 < z < 1.3$ taken from one of the $1^\circ \times 1^\circ$ Canada–France–Hawaii Telescope Legacy Survey Deep Fields. We parametrize galaxy morphology according to the Sérsic index n , taking $n > 2$ to be “bulge-dominated” and $n < 2$ to be “disk-dominated”. Our $n > 2$ number fractions at $z = 0.1$ agree well with those based on Sloan Digital Sky Survey galaxies. We find that the $n > 2$ galaxy number fraction is constant with redshift in the field. However, for overdense environments this fraction is larger and increases towards lower redshifts, higher densities and higher luminosities. Rest-frame color-magnitude diagrams show that the color distribution is bimodal out to our redshift limit of $z \sim 1$ with a prominent red-sequence of galaxies at $0.2 < z < 0.4$ and a large blue-peak dominance at $0.8 < z < 1$. We use this bimodality to define a red fraction as the fraction of galaxies having a rest-frame color $u^* - g' > 1$. For all environments, this fraction increases towards lower redshifts and higher luminosities. The red fraction within cluster-like regions changes 60% faster with redshift as compared to the field for galaxies with $M_{g'} < -19.5$. Using, for the first time, observations across many cluster-field interfaces distributed over a single, large volume, we trace the large-scale morphology-density relation and the Butcher-Oemler effect over a period of almost 8 Gyr.

¹This work is based in part on data obtained as part of the Canada-France-Hawaii Telescope Legacy Survey, a collaborative project of the National Research Council of Canada and the French Centre national de la recherche scientifique.

²Leiden Observatory, P.O. Box 9513, NL-2300 RA, Leiden, The Netherlands.

³National Research Council of Canada, Herzberg Institute of Astrophysics, 5071 West Saanich Road, Victoria, BC V9E 2E7, Canada.

⁴Department of Physics & Astronomy, University of Victoria, P.O. Box 3055, Victoria, BC V8W 3P6, Canada.

⁵Guest User, Canadian Astronomy Data Centre, which is operated by the Dominion Astrophysical Observatory for the National Research Council of Canada’s Herzberg Institute of Astrophysics.

Subject headings: galaxies: morphology — galaxies: formation — galaxies: evolution — galaxies: statistics — cosmology: observations

1. Introduction

Galaxy populations show great diversity in morphologies and colors (e.g., Hubble 1926). Many studies of the local and high-redshift universe show that there exist strong relations between galaxy morphology, color and environment (e.g., Dressler 1980; Kennicutt 1983; Whitmore et al. 1993; Dressler et al. 1997; Hogg et al. 2003).

In order to explain the observed correlations, current theories of galaxy formation and evolution adopt a Λ -dominated cold dark matter model for the universe where large-scale structure is built through hierarchical clustering of dark matter halos. Early-type galaxies are then assembled through the (successive) merging of disks that formed in these halo's. An important test of this formation scenario is to trace and quantify the redshift evolution of observable galaxy properties as a function of environment. Significant progress has recently been made on this issue with the availability of large and homogeneous datasets for direct comparisons with theoretical predictions. For example, the Sloan Digital Sky Survey (SDSS; Stoughton et al. 2002) has been used at the low redshift end ($z \sim 0.1$) to study various correlations between observable galaxy properties and the larger scale environment (Goto et al. 2003; Hogg et al. 2004). At higher redshifts, Bell et al. (2004) were able to put strong constraints on hierarchical formation models by exploring the rest-frame properties of color-selected early-type galaxies as function of redshift. In this Letter, we include galaxy environment as another important variable in the evolutionary signatures predicted by the hierarchical models. Taking the SDSS as baseline (Hogg et al. 2004) we examine both the morphology (bulge- vs. disk-dominated) and rest-frame color (red vs. blue) redshift evolution of galaxies residing within different environments from the field to massive clusters. We make use of data from the Canada–France–Hawaii Telescope Legacy Survey (CFHTLS) which is well suited to address these issues as its extensive sky coverage provides large, homogeneous and statistically well-defined samples of galaxies spanning a wide range of redshifts and densities.

This Letter is organized as follows: Section 2 describes the CFHTLS-Deep data, and Section 3 outlines the morphology and environment analysis. In Section 4, we present and discuss our results. The cosmological parameters adopted throughout this Letter are $H_0 = 70 \text{ km s}^{-1} \text{ Mpc}^{-1}$, and $(\Omega_M, \Omega_\Lambda, \Omega_k) = (0.3, 0.7, 0.0)$.

2. The Data

The CFHTLS-Deep survey consists of $u^*g'r'i'z'$ images of four uncorrelated areas of the sky taken with the MegaPrime prime focus mosaic imager (thirty-six 2080x4622 chips). Each patch covers about $1^\circ \times 1^\circ$ and is located away from the galactic plane in order to minimize galactic extinction and bright star contamination. When completed, the Deep Survey will produce images almost as deep as the Hubble Deep Field (Williams et al. 1996) but covering an area of the sky 3500 times as large. The data used here are from the CFHTLS-D3 field (RA(2000) = $14^h 19^m 28^s$, DEC(2000) = $+52^\circ 40' 41''$) after one year of observing. D3 was chosen because it overlaps with a Canada-France Redshift Survey field (Lilly et al. 2001) and partially with the “Groth Strip” (Groth et al. 1994; Rhodes et al. 2000). We thus have 338 spectroscopic redshifts available from the literature for calibrating our photometric redshifts.

The data were processed (de-biased, flat-fielded, fringe-corrected, etc.) through the Elixir pipeline (Magnier & Cuillandre 2004) and retrieved from the Canadian Astronomical Data Centre (CADC). All the images were astrometrically and photometrically calibrated and then stacked (Gwyn et al., in preparation). The final photometric zero-point uncertainties are less than 0.05 mag. The galaxy photometry package SExtractor (Bertin & Arnouts 1996) was used to detect objects in the i' -band and to perform photometry using Kron (1980) apertures.

3. Analysis

3.1. Photometric Redshifts

Photometric redshifts and spectral types were determined (Gwyn et al., in preparation). Based on a comparison with the available spectroscopic redshifts, the typical relative photometric redshift error is $\delta z/(1+z) = 0.11$. Using the best-fit photometric redshift and spectral type, we calculated k -corrections and $u^*g'r'i'z'$ rest-frame galaxy AB absolute magnitudes. The maximum accessible volume V_{acc} (Schmidt 1968) was also computed for each object (Gwyn et al., in preparation) by determining the redshift range over which its magnitude would fall within the i' -band limiting magnitude of the sample ($i' < 24.5$ mag). Galaxies were then weighted by the resulting $1/V_{acc}$ values to compute number densities in the color-magnitude plane.

3.2. Quantitative Morphologies

We measured the structural parameters of our galaxies in the i' -band in a quantitative, uniform and reproducible way using the GIM2D package (Simard et al. 2002). We fit two-dimensional, PSF-convolved, pure Sérsic models of the form $\Sigma(r) = \Sigma_0 \exp(-r/r_0)^{1/n}$ to our galaxy images. The shape or concentration parameter n is known as the “Sérsic index” (Sérsic 1968). The choice of such a simple model was better suited to the spatial resolution of our ground-based data than a full, more complex bulge+disk decomposition. Spatially-varying point-spread-functions (FWHM $\sim 0''.7 - 0''.9$) were constructed across each MegaPrime chip directly from stars in the images using the DAOPHOT package (Stetson 1987). The galaxy total flux (F_{tot}) and *intrinsic* half-light radius $r_{1/2}$ were obtained by integrating the best-fit GIM2D Sérsic model out to $r = \infty$. Absolute rest-frame total g' -band magnitudes ($M_{g'}$) were calculated for the best-fit models from the apparent and absolute aperture magnitudes.

Following Simard et al. (2002) we conducted extensive simulations in order to characterize the systematic biases and random errors in the GIM2D/CFHTLS-D3 i' -band structural measurements. After careful inspection of our simulation results, we concluded that the sample we will use with $i'_{model} < 24$ mag (1) has a completeness of $\sim 98.5\%$ and (2) has combined random and systematic errors of $\Delta n \sim 0.76$ for $r_{1/2} > 0''.1$.

3.3. Overdensity Estimator δ_{15th}

A total of 65,624 galaxies with $i' < 24.5$ mag and $0 < z < 1.3$ were used for our overdensity calculations. For each galaxy we estimate the overdensity of its environment relative to mean density at its redshift using the projected distance, r_{15th} , to the fifteenth nearest galaxy. The overdensity is then defined as the ratio of the galaxy number density within a cylinder of length dD_L and radius r_{15th} centered at the galaxy over the mean number density:

$$\delta_{15th} = (15 / \alpha \pi r_{15th}^2 dD_L) / (N_{tot} / V_{tot}), \quad (1)$$

where α is an areal correction factor for the edges of the MegaPrime detectors, dD_L is the luminosity distance interval corresponding to a redshift interval centered at the galaxy, N_{tot} and V_{tot} are the total number of galaxies and total volume within the effective MegaPrime field ($\sim 0.9 \text{ deg}^2$) of the same redshift interval.

An important issue is to properly take into account inaccuracies introduced by the usage of the photometric redshift. We address this by first assuming that each z_{phot} value has an associated Gaussian error probability distribution. Each galaxy is then successively placed in the center of five adjacent redshift bins with the central bin at z_{phot} and the outermost

bins benchmarking the 99% confidence level. We adopt $\delta z/(1+z) = 0.11$ as the redshift uncertainty estimator. All five δ_{15th} 's are weighted by the Gaussian probability distribution and averaged to yield one final overdensity estimate for each galaxy. Monte Carlo simulations show that nearly 70% of the galaxies have a measurement error on δ_{15th} smaller than 0.3 (68% confidence level).

4. Results and Discussion

We selected all galaxies with $r_{1/2} > 0''.1$ and $M_{g'} \leq -19.5$ mag (corresponding to $i'_{model} \sim 24$ at $z \sim 1$) to keep only galaxies with reliable structural parameters (see §3.2). Due to low number statistics we adopt a lower redshift limit of 0.2. Furthermore we exclude $z > 1$ objects due to their large uncertainties in z_{phot} . These cuts leave us with an essentially volume-limited sample of 28,911 galaxies with $0.2 < z < 1$ which we divide into 4 equal redshift bins. Figure 1 shows the $1/V_{acc}$ weighted rest-frame color-magnitude diagrams for the lowest ($0.2 < z < 0.4$) and highest ($0.8 < z < 1$) redshift bins as function of morphology and environment. Figure 2 shows the redshift evolution of the number fractions of $n > 2$ (“bulge-dominated”) galaxies and red (rest-frame¹ $u^* - g' > 1$) galaxies as a function of luminosity² and environment. We stress the quantitative nature of our morphological classification scheme in that it measures the concentration of the galaxy light profiles as parameterized by the Sérsic index n . We chose $n = 2$ as our morphological discriminator between “bulge” and “disk” dominated galaxies to be fully consistent with Hogg et al. (2004) who studied similar morphology-color-magnitude relations for SDSS galaxies ($\bar{z} \sim 0.1$). Their results are also plotted in Figure 2a. We find good quantitative agreement (within the errors) for our $M_{g'} < -20$ number fractions when extrapolated down to the SDSS redshift of $z \sim 0.1$. We summarize our main results as follows:

1. Within the entire $M_{g'} < -19.5$ sample the $n > 2$ galaxy number fraction remains constant with redshift to within $\sim 10\%$ (see Fig. 2a). At all redshifts, field populations have the lowest $n > 2$ fraction and this fraction remains constant with redshift. However, for overdense environments this fraction is larger and consistently increases towards lower redshifts, higher densities and higher luminosities showing that a strong morphological evolution has taken place since $z \sim 1$. In overdense regions we observe that for $0.2 < z < 1$

¹In the remainder of this Letter we will use the $u^* - g'$ color always as being defined in the rest-frame of the galaxy.

²To avoid too small number statistics we take cumulative lower absolute magnitude limits instead of fixed absolute magnitude bins.

the “bulge-” vs. “disk-dominated” galaxy ratio has increased by as much as a factor of ~ 2 among bright $M_{g'} < -22$ populations relative to $M_{g'} < -19.5$ populations.

2. At all redshifts, cluster-like environments also contain the highest fraction of red ($u^* - g' > 1$) galaxies. With mostly blue ($u^* - g' < 1$) galaxies at $z \sim 1$, the red fraction increases towards lower redshifts and higher luminosities. The red fraction within cluster-like regions changes faster with redshift as compared to the field. We quantify this by fitting a line with slope β to the observed color evolutions and find $\beta_{\delta > 2} / \beta_{\delta < 1} \sim 1.6$ for $M_{g'} < -19.5$. We note the presence of a break at $z \sim 0.7$ which marks a period of a less strong ($\sim 35\%$) color evolution down to $z = 0.2$.

The results discussed in 1 and 2 qualitatively agree with the postulations and predictions made by hierarchical formation models (e.g. Kauffmann & Charlot 1998; Cole et al. 2000) where galaxies are initially formed as blue star-forming systems with $n < 2$ or “disk-dominated” profiles. The observed trends show that the onset of a population’s morphological evolution depends strongly on environment with the cluster-like environments exhibiting the strongest evolution. The latter would indicate that “bulge-dominated” galaxies are assembled at earlier times in denser environments which is in agreement with the predictions made by hierarchical merging models (e.g., Benson et al. 2000; Berlind et al. 2003). More specifically, they predict that mergers erase any galaxy disk signatures and lead to more spheroidal structures such as bulges (e.g., Barnes & Hernquist 1996) and that higher merger rates associated with denser environments (e.g., Lacey & Cole 1993) result in earlier onsets of morphological transformation. Mergers also lead to increased galaxy luminosity through the addition of stellar mass and ultimately result in more luminous and “bulge-dominated” populations. Our observations support this merging scenario.

3. In all environments, the color distribution of the observed galaxies is bimodal out to $z \sim 1$ with a ‘gap’ at $u^* - g' \sim 1$ which is in agreement with the observations of Bell et al. (2004). Rest-frame color-magnitude diagrams (Fig. 1) show that there exists a prominent red-sequence of galaxies at $0.2 < z < 0.4$ and a large blue-peak dominance at $0.8 < z < 1$. Equivalent color-magnitude diagrams for the redshift range $0.4 < z < 0.8$ (not included here) show bimodal distributions intermediate between these low and high redshift bins. The red peak ($u^* - g' > 1$) of this bimodality appears to be greatly reduced towards higher redshifts and is predominantly being ‘built up’ from “bulge-dominated” galaxies with decreasing redshift. This build-up proceeds more rapidly in more overdense environments.

Based on their examination of the color bimodality, Bell et al. (2004) concluded that a combination of the interaction/merging of passively evolving galaxies and the truncation of their star formation would explain the main features of their observed color distribution. They suggest that the truncation may be associated with mergers that consume all the gas

in an induced starburst. It is therefore interesting that we observe a strong color-magnitude relation (brighter being redder) at all redshifts and within all environments with a clear increase of the color evolutionary rate towards denser environments. The latter would agree well with an enhanced truncation of the star formation within denser environments. In addition to higher merger rates, denser environments also have other processes such as ram-pressure and that can affect galaxies travelling through their hot intergalactic medium (e.g., Quilis et al. 2000; Bekki et al. 2002).

The picture emerging from results presented here and elsewhere is one that supports basic tenets of hierarchical galaxy formation and evolution. The CFHTLS-Deep is an ongoing project, and the final dataset will allow us to quadruple our sample size with even greater sky coverage and depth. As is, our results show for the first time the redshift evolution of the color-magnitude-morphology relation over a single cosmological volume large enough to encompass many different environments ranging from the field to the most massive clusters.

We would like to thank CFHT staff and members of the CFHTLS community involved in the planning and execution of survey observations and data processing. M. J. H. M. N. would especially like to thank the Herzberg Institute of Astrophysics (NRC-HIA) for their hospitality and financial support during the time when this work was conducted.

REFERENCES

- Barnes, J. E., & Hernquist, L. 1996, *ApJ*, 471, 115
- Bekki, K., Couch, W. J., & Shioya, Y. 2002, *ApJ*, 577, 651
- Bell, E. F., et al. 2004, *ApJ*, 608, 752
- Benson, A. J., Baugh, C. M., Cole, S., Frenk, C. S., Lacey, C. G. 2000, *MNRAS*, 316, 107
- Berlind, A. A., et al. 2003, *ApJ*, 593, 1
- Bertin, E., & Arnouts, S. 1996, *A&A*, 117, 393
- Cole, S., Lacey, C. G., Baugh, C. M., Frenk, C. S. 2000, *MNRAS*, 319, 168
- Dressler, A. 1980, *ApJ*, 236, 351
- Dressler, A., et al. 1997, *ApJ*, 490, 577

- Goto, T., Yamauchi, C., Fujita, Y., Okamura, S., Sekiguchi, M., Smail, I., Bernardi, M.
MNRAS, P. L. 2003, MNRAS, 346, 601
- Groth, E. J. et al. 1994, BAAS, 185, 5309
- Hogg, D. W., et al. 2003, ApJ, 585, 5
- Hogg, D. W., et al. 2004, ApJ, 601, 29
- Hubble, E. P. 1926, ApJ, 64, 321
- Kauffmann, G., & Charlot, S. 1998, MNRAS, 294, 705
- Kennicutt, R. C., Jr. 1983, AJ, 88, 483
- Kron, R. G. 1980, ApJS, 43, 305
- Lacey, C., & Cole, S. 1993, MNRAS, 262, 627
- Lilly, S. J., Le Fevre, O., Crampton, D., Hammer, F., Tresse, L. 2001, ApJ, 455, 50
- Magnier, E. A., & Cuillandre J. C. 2004, PASP, 116, 449
- Quilis, V., Moore, B., & Bower, R. 2000, Science, 288, 1617
- Rhodes, J., Refregier, A., & Groth, E. J. 2000, ApJ, 536, 79
- Schmidt, M. 1968, ApJ, 151, 393
- Sérsic, J. L. 1968, Atlas de Galaxias Australes (Cordoba: Obs. Astron.)
- Simard, L., et al. 2002, ApJS, 142, 1
- Stetson, P. B. 1987, PASP, 99, 191
- Stoughton, C., et al. 2002, AJ, 123, 485
- Whitmore, B. C., Gilmore, D. M., & Jones, C. 1993, ApJ, 407, 489
- Williams, R. E. et al. 1996, AJ, 112, 1335

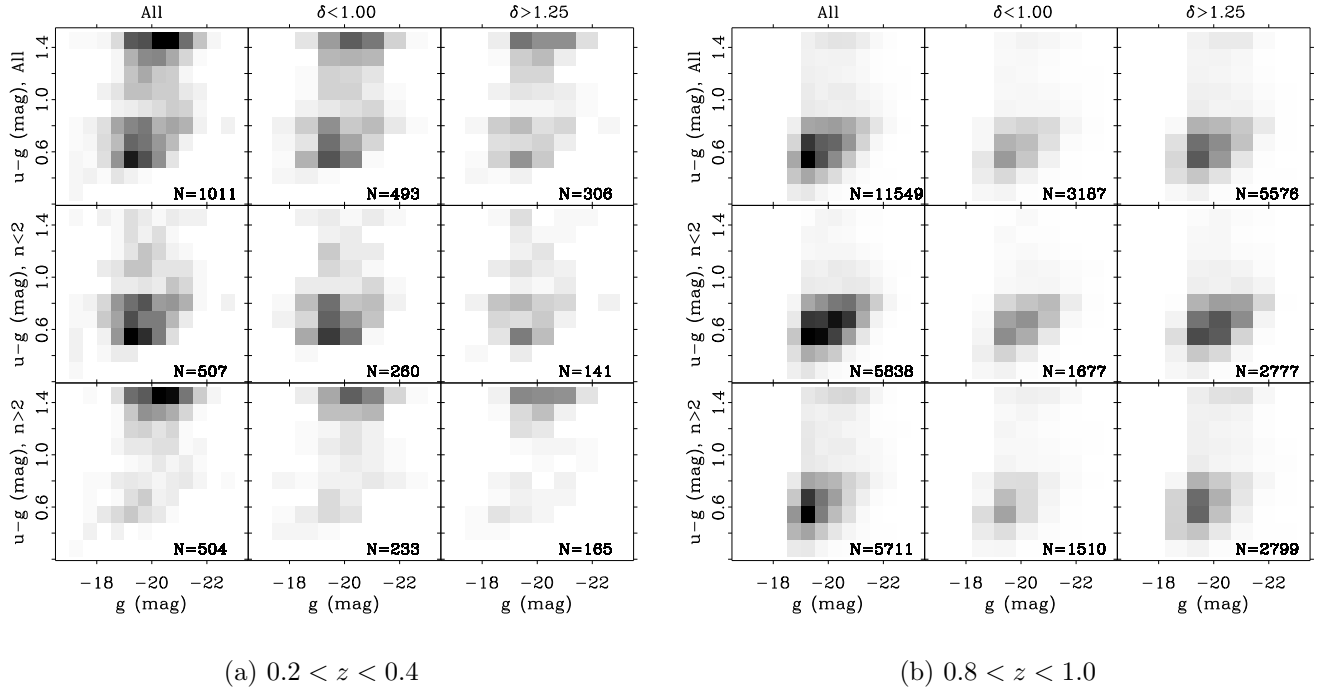


Fig. 1.— $1/V_{acc}$ weighted rest-frame color-magnitude diagrams for all galaxies with $M_{g'} < -19.5$ as function of the overdensity estimator δ_{15th} (rows) and Sérsic index n (columns) for (a) $0.2 < z < 0.4$ and (b) $0.8 < z < 1.0$. In each panel the grey scale monotonically represents the number densities of galaxies in the two-dimensional space of color and magnitude (for each row normalization w.r.t. to the highest value bin of the *left* panel). Equivalent color-magnitude diagrams for the redshift range $0.4 < z < 0.8$ (not included here) show bimodal distributions intermediate between (a) and (b).

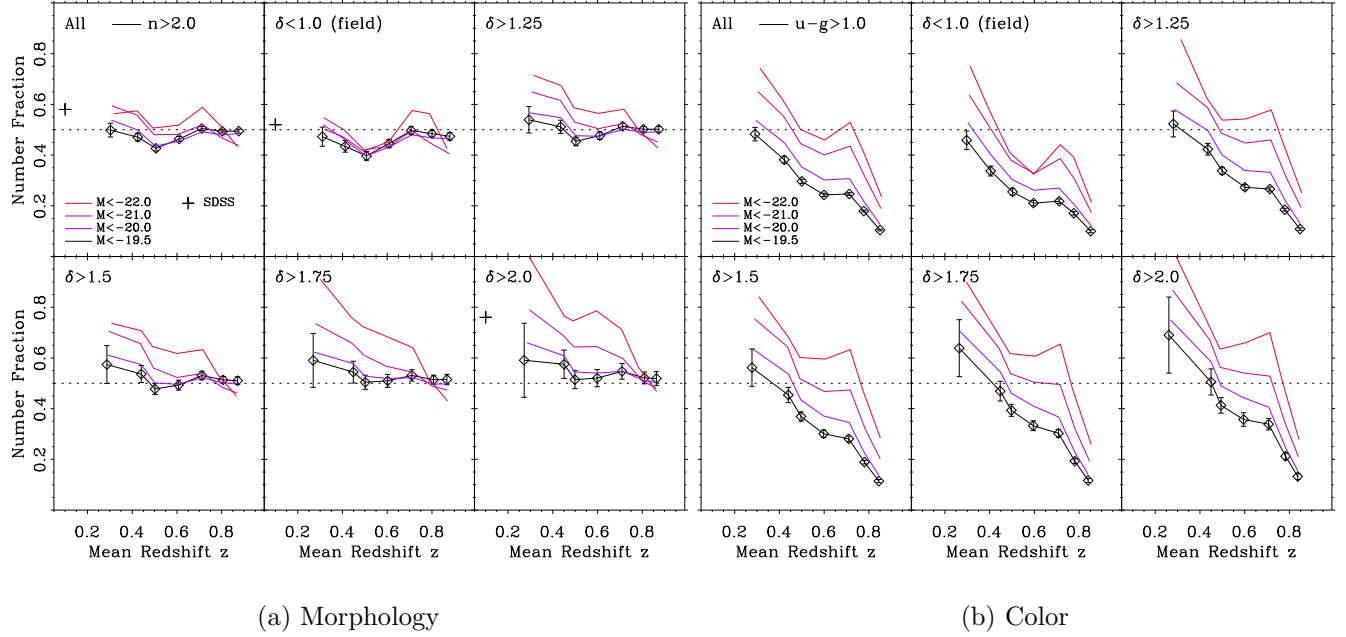


Fig. 2.— The observed evolution of galaxies out to $z \sim 1$ in terms of galaxy number fractions for (a) morphology and (b) color as function of galaxy total luminosity $M_{g'}$ and the overdensity estimator δ_{15th} . Panel (a) shows the number fractions for $n > 2$ galaxies (Sérsic index n). The crosses are the $n > 2$ number fractions based on SDSS galaxies. Panel (b) shows the number fractions for red galaxies (rest-frame $u^* - g' > 1$). The fractions are calculated for seven redshift bins with increments of 0.1 and fixed widths of 0.2. The error bars are given by Poisson statistics only and are shown only for $M_{g'} < -19.5$ for clarity.